Supporting Information: Primary Product Branching in the Photodissociation of Chloroacetaldehyde at 157 nm

Jonathan D. Adams, Preston G. Scrape, Shenshen Li, Shih-Huang Lee,[‡] and Laurie J. Butler*

[‡]National Synchrotron Radiation Research Center, Hsinchu 30076, Taiwan, Republic of China

**The James Franck Institute and Department of Chemistry, The University of Chicago, Chicago, Illinois 60637 USA*

Contents

A. Molecular Beam Speed Distribution

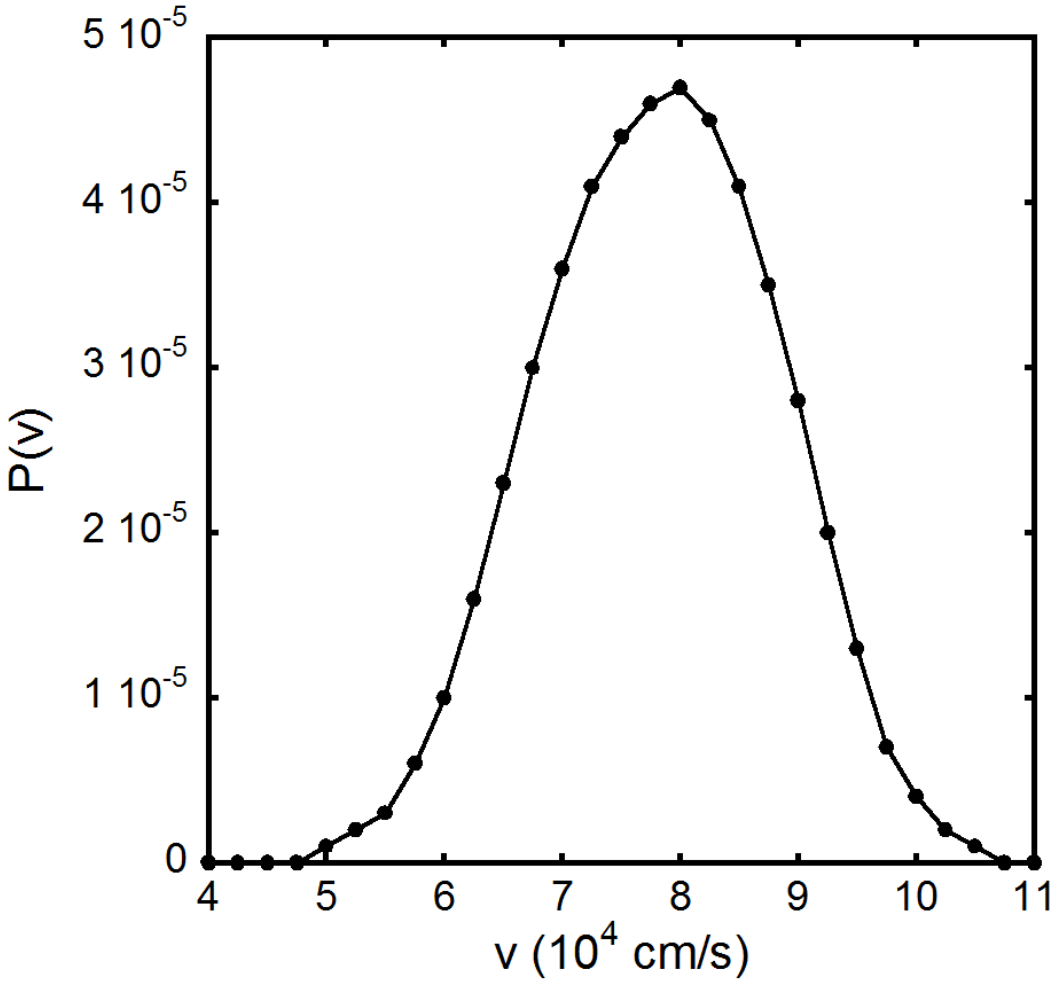

Figure S.1: Molecular beam speed distribution used to fit the time-of-flight data. This distribution was derived from the measured number density distribution obtained in a hole burning experiment after accounting for the on-axis contribution from the monomer produced in the photodissociation of molecular clusters.

B. Alternative Fits to the *m/z* = 35 and *m/z* = 36 TOF Spectra Using the C–Cl Bond Fission P(E_T) Derived in the Velocity Map Imaging Study

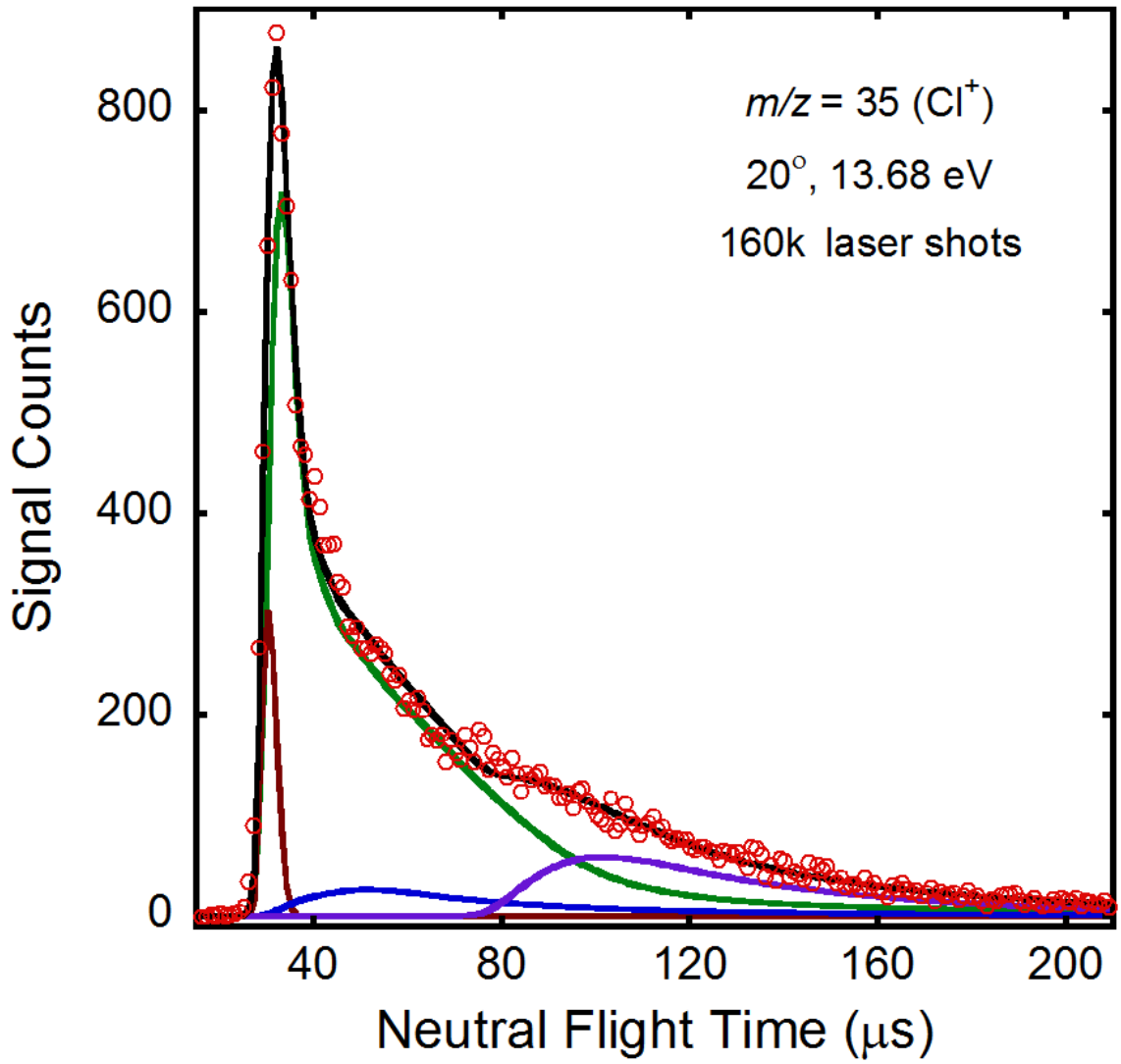

Figure S.2: TOF spectrum taken at *m/z* = 35 (Cl^+) with a source angle of 20° and an ionization energy of 13.68 eV. Data are shown in red circles. Primary C–Cl bond fission is fit by the solid green line using the C–Cl bond fission P(E_T) derived in the velocity map imaging study (see Figure 4 in Reference 5). The contribution from bleed in of *m/z* = 36 (Cl^+) is shown in solid blue line and is fit using the primary HCl photoelimination P(E_T) shown in Figure 2. The fit shown as the solid purple line represents the contribution attributed to photodissociation of clusters in the molecular beam. The fast signal is fit as Cl loss from the dimer hydrate of chloroacetaldehyde. This fit, shown in solid maroon line, is derived the P(E_T) shown in Figure S.3.

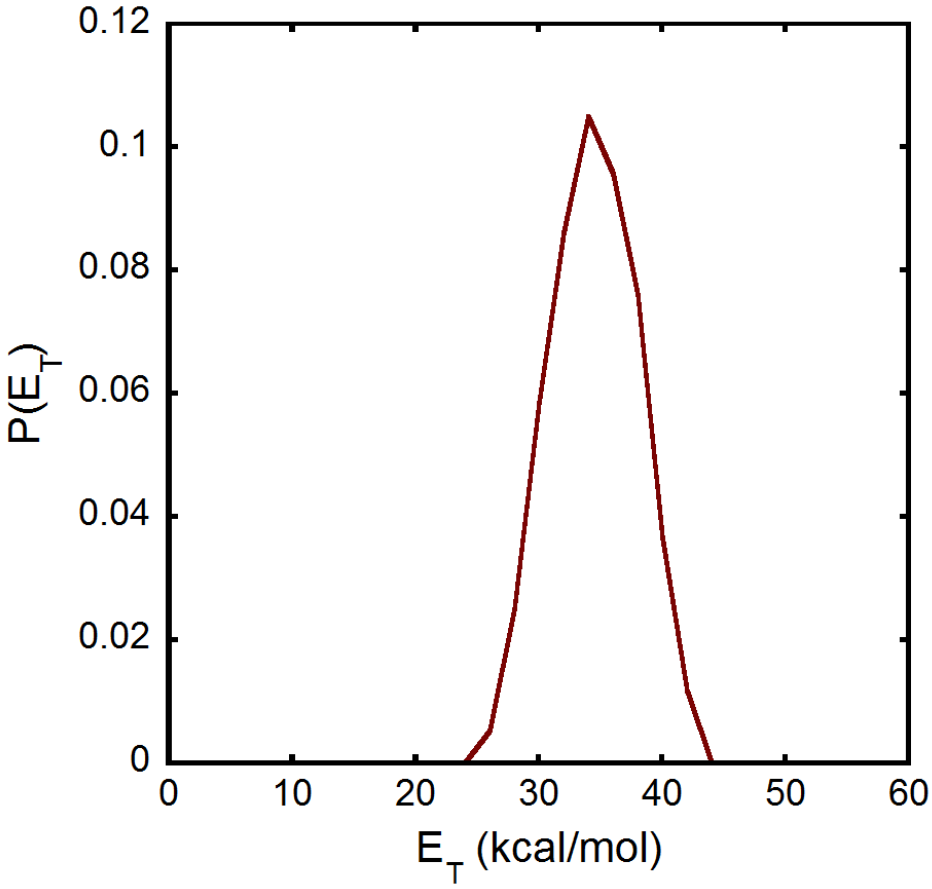

Figure S.3: Photofragment recoil kinetic energy distribution for C–Cl bond fission assuming the fastest signal results from photodissociating the dimer hydrate of chloroacetaldehyde at 157 nm. The P(E_T), peaking at 34 kcal/mol, is derived by forward convolution fitting of the fastest signal in the TOF spectrum taken at *m/z* = 35 (Cl^+) shown in Figure S.2.

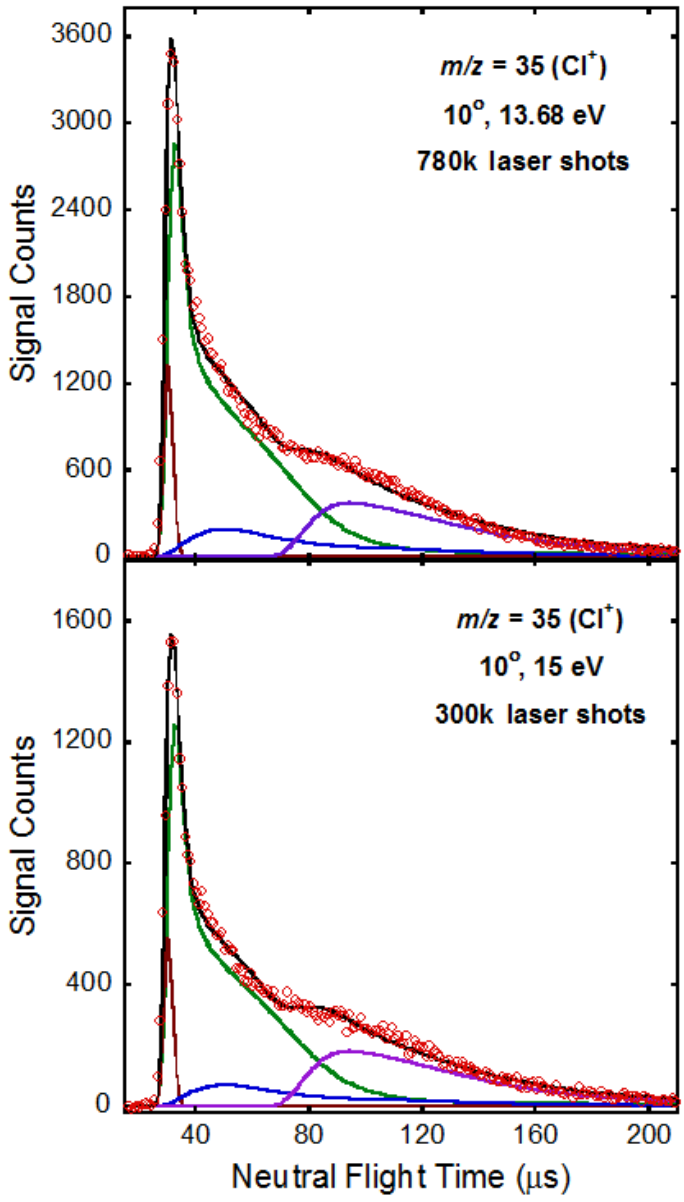

Figure S.4: TOF spectrum taken at *m/z* = 35 (Cl^+) with a source angle of 10° and two different ionization energies. The upper frame shows the data taken at an ionization energy of 13.68 eV and the lower frame shows the data taken at an ionization energy of 15.0 eV. Data are shown in red circles. Primary C–Cl bond fission is fit by the solid green line using the C–Cl bond fission P(E_T) derived in the velocity map imaging study (see Figure 4 in Reference 5). The contribution from bleed in of *m/z* = 36 ($H^{35}Cl^+$) is shown in solid blue line and is fit using the primary HCl photoelimination P(E_T) shown in Figure 2. The fit shown as the solid maroon line corresponds to Cl loss from the dimer hydrate of chloroacetaldehyde and is derived the P(E_T) shown in Figure S.3. The fit shown as the solid purple line represents the contribution attributed to photodissociation of clusters in the molecular beam.

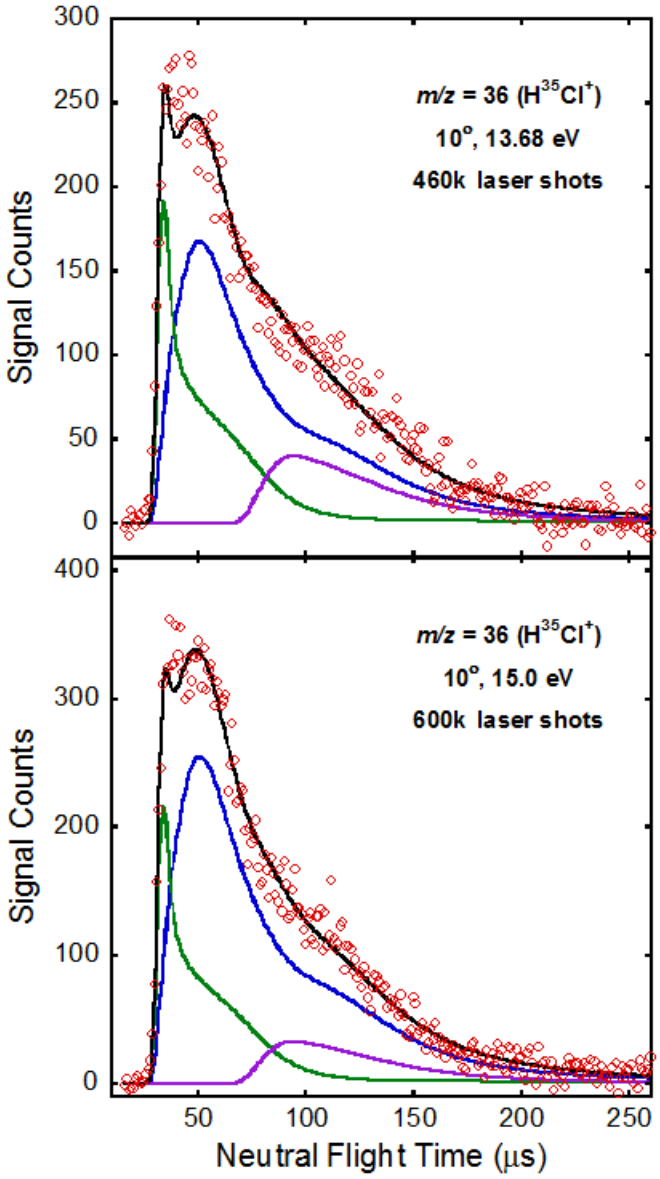

Figure S.5: TOF spectrum taken at *m/z* = 36 ($H^{35}Cl^+$) with a source angle of 10° and two different ionization energies. The upper frame shows the data taken at an ionization energy of 13.68 eV and the lower frame shows the data taken at an ionization energy of 15.0 eV. Data are shown in red circles. Primary HCl photoelimination is fit by the solid blue line using the P(E_T) shown in Figure 2. The contribution from bleed in of *m/z* = 37 (Cl^+) is shown in solid green line and is fit using the primary C–Cl bond fission P(E_T) derived in the velocity map imaging study (see Figure 4 in Reference 5). The contribution attributed to photodissociation of clusters in the molecular beam is shown in solid purple line. While we get a better fit to the fast signal in both of these TOF spectra, the contribution of bleed in from *m/z* = 37 (Cl^+) is much larger than expected based on the signal observed in the *m/z* = 37 (Cl^+) TOF data.

C. Further Details on Branching Calculations

Using our branching calculations, we first determined the portions of the primary C−Cl bond fission P(E_T), shown in green line in Figure 4, that produces vinoxy that we expect to dissociate to H + ketene or CH_3 + CO products respectively. To summarize, the branching calculations assume that the unimolecular dissociation of vinoxy occurs on the ground state PES and that the excitation of the photolytic precursor is to an excited-state PES of chloroacetaldehyde that is repulsive along the C−Cl bond in the Franck-Condon region. The inputs for the branching calculations include the geometry of chloroacetaldehyde and vinoxy, the experimentally determined C−Cl bond fission P(E_T), the vibrational normal modes of vinoxy at its minimum geometry and at each transition state, the nozzle temperature, and the barrier heights for the H + ketene and isomerization channels. Since the barrier to CH_3 + CO from the acetyl radical is much lower than the barrier to isomerization (see Figure 1 in Reference 5), we use the isomerization barrier height in the calculations and assume all radicals that undergo isomerization subsequently dissociate to CH_3 + CO. To account for the different conformers for chloroacetaldehyde, we scale the C−Cl bond fission P(E_T) by the relative population of each conformer in the molecular beam at the nozzle temperature, run the branching calculations for each conformer separately, and then sum their contributions. Because the scattering instrument uses single photon photoionization rather than REMPI, we were unable to detect the separate spin-orbit states of the Cl atoms from primary C−Cl bond fission and therefore we do not distinguish between the separate states in our branching calculations (see Chapter 3 in Reference 21). In the velocity map imaging study,[5] we found a barrier height of 44.6 kcal/mol for the H + ketene channel to be more consistent with the data than the G4 barrier height (42.2 kcal/mol). The results of the branching calculations are shown in Figure 8 along with the total C−Cl bond fission P(E_T) from Figure 4 shown in solid green line. The dashed red line shows the portion of the C−Cl bond fission P(E_T) producing vinoxy which dissociates to H + ketene and the dashed blue line shows the portion producing vinoxy which dissociates to CH_3 + CO (here we assume that all the Cl atom signal fit in green in the TOF spectra are produced from the single photon photodissociation of chloroacetaldehyde, although there may be a contribution from multiphoton dissociation at the earliest arrival times in the TOF spectrum). We also show the portion predicted to produce stable vinoxy radicals in dashed gray line, which we used to fit the contributions from dissociation ionization or multiphoton dissociation of vinoxy.

D. Critical Points on the Potential Energy Surface of the HCCHO Radical

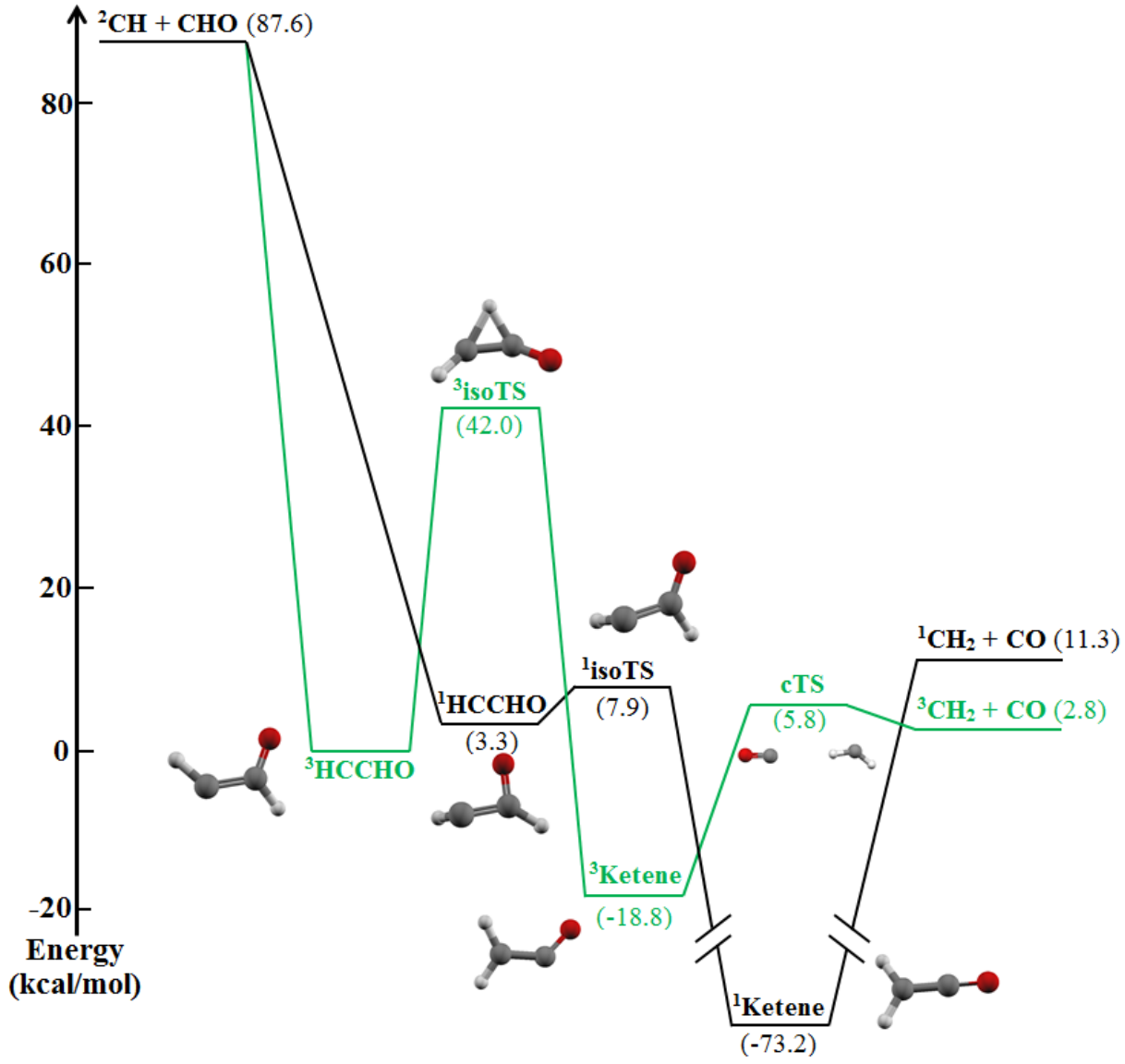

Figure S.6: Selected minima and transition states on the singlet (black) and triplet (green) potential energy surfaces of HCCHO radical. The energies of the stationary points relative to the zero-point level of ground state triplet HCCHO are given in parentheses. They are calculated at the G4//B3LYP/6-311G++(3df,2p) level of theory and include zero-point energy corrections.

E. Calculation of Branching Ratios Between Primary Photodissociation Channels Using the C–Cl Bond Fission P(E_T) From the Velocity Map Imaging Study

Here we recalculate the branching ratios between the primary photodissociation channels using the C–Cl bond fission P(E_T) from the velocity map imaging study. The purpose of these calculations is to gauge the possible error introduced in the characterization of the primary product branching by attributing the fast signal in the *m/z* = 35 (Cl^+) TOF spectra to C–Cl bond fission. While we use the same *m/z* = 35 (Cl^+) TOF data to calculate these branching ratios, we are not attributing the same signal to C–Cl bond fission (Figures S.2 and S.4). Since we specifically want to see the effect from different fitting methods to the *m/z* = 35 (Cl^+) data, we did not alter the fits to the *m/z* = 36 ($H^{35}Cl^+$) and *m/z* = 49 (CH_2Cl^+) TOF data used in these calculations. We obtain

$$\frac{\Phi_{\text{C-Cl}}}{\Phi_{\text{HCl}}} = \text{obs}\left(\frac{^{35}\text{Cl}^+}{\text{H}^{35}\text{Cl}^+}\right) \times \text{TS}\left(\frac{\text{H}^{35}\text{Cl}}{^{35}\text{Cl}}\right) \times \left(\frac{\sigma_{\text{HCl/HCl}^+}}{\sigma_{\text{Cl/Cl}^+}}\right) = \left(\frac{69011}{13813}\right) \times \left(\frac{139876}{66299}\right) \times \left(\frac{16\ \text{Mb}}{22.8\ \text{Mb}}\right) = 7.4,$$

and

$$\frac{\Phi_{\text{C-Cl}}}{\Phi_{\text{C-C}}} = \text{obs}\left(\frac{^{35}\text{Cl}^+}{\text{CH}_2\text{Cl}^+}\right) \times \text{TS}\left(\frac{\text{CH}_2\text{Cl}}{^{35}\text{Cl}}\right) \times \left(\frac{\sigma_{\text{CH}_2\text{Cl/CH}_2\text{Cl}^+}}{\sigma_{\text{Cl/Cl}^+}}\right) = \left(\frac{17805}{30371}\right) \times \left(\frac{33445}{11488}\right) \times (1.17) = 2.0.$$

The combination of these two ratios yields total primary photodissociation branching fractions for C–Cl fission:HCl photoelimination:C–C fission of 0.61:0.083:0.31. Overall, attributing the additional fast signal in the *m/z* =35 (Cl^+) data to C–Cl bond fission introduces an uncertainty of about 18% to the branching ratios. However, the branching fractions between all three primary channels do not change significantly and therefore the possibility of multiphoton dissociation events introduces minimal changes to the observed branching.

F. Isotope Dependence of the HCl Photoelimination TOF Data

Although we accounted for the bleed in from *m/z* = 36 ($H^{35}Cl^+$) into the TOF spectrum of *m/z* = 35 (Cl^+) using the HCl photoelimination P(E_T) derived from the TOF spectrum of *m/z* = 38 ($H^{37}Cl^+$), we note that there are a few inconsistencies between the *m/z* = 36 and *m/z* = 38 data. Figure S.7 shows the TOF spectra collected at *m/z* = 36 ($H^{35}Cl^+$) with a source angle of 10° and ionization energies of 15 eV (top frame) and 13.68 eV (bottom frame). In both spectra, we show the fits derived from the HCl photoelimination P(E_T), shown in Figure 2, in solid blue line. Not only does there appear to be extra fast signal that cannot be accounted for using the P(E_T), but it also appears as though the fast signal does not show the same dependence on ionization energy as the signal attributed to HCl photoelimination. While we expect bleed in from *m/z* = 37 (Cl^+), the signal from that process is too fast and cannot account for the entire fast signal in the *m/z* = 36 TOF spectra. It is possible that $H^{35}Cl$ elimination has a slightly different P(E_T) than does $H^{37}Cl$ elimination, but the signal at *m/z* = 38 for the latter is uncomplicated by the low quadrupole resolution so we present a P(E_T) derived from the *m/z* = 38 TOF spectrum. While it would be more accurate to incorporate all of the signal from the *m/z* = 36 data to the bleed in observed in the *m/z* = 35 TOF spectrum, we note that doing so does not significantly alter the fits. Therefore, we use the P(E_T) depicted in Figure 4 and note that we may be overestimating the amount of C−Cl bond fission events. We thus expect the branching ratios calculated in Equations (4) and (5) to be maximum values such that there may be more HCl photoelimination and C−C bond fission events relative to C−Cl bond fission. For comparison, we present the same calculations using the C−Cl bond fission P(E_T) determined in the velocity map imaging study (shown in black line in Figure 4) in the Supporting Information.

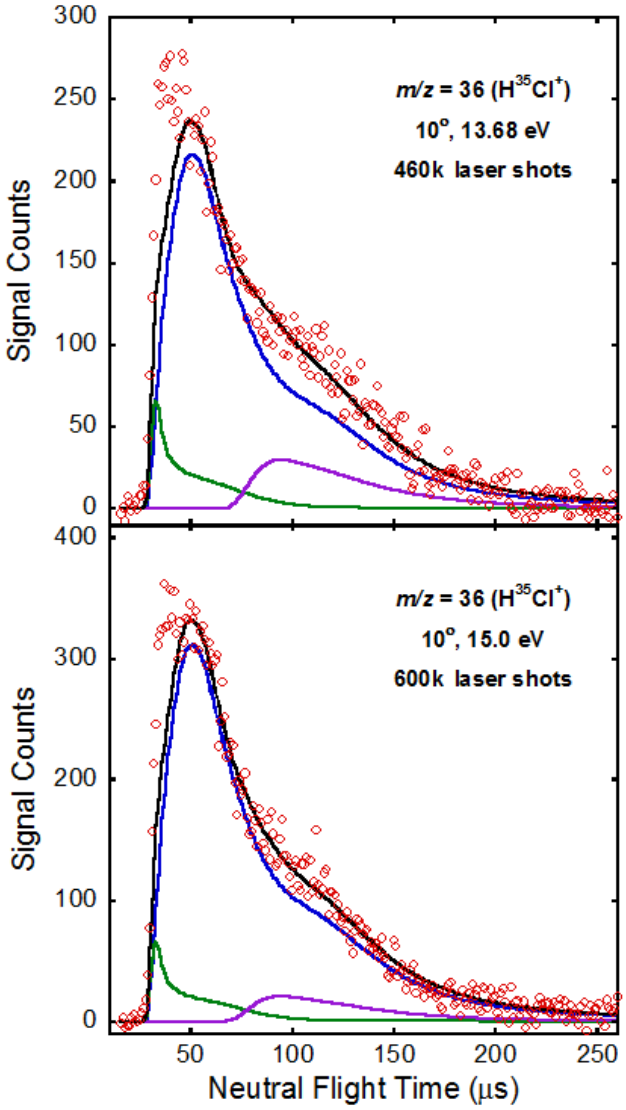

Figure S.7: TOF spectrum taken at *m/z* = 36 ($H^{35}Cl^+$) with a source angle of 10° and two different ionization energies. The upper frame shows the data taken at an ionization energy of 13.68 eV and the lower frame shows the data taken at an ionization energy of 15.0 eV. Data are shown in red circles. Primary HCl photoelimination is fit by the solid blue line using the P(E_T) shown in Figure 2. The contribution from bleed in of *m/z* = 37 (Cl^+) is shown in solid green line and is fit using the primary C−Cl bond fission P(E_T) shown in solid green line in Figure 4. The contribution attributed to photodissociation of clusters in the molecular beam is shown in solid purple line. It is interesting to note that the primary HCl photoelimination P(E_T) derived from the TOF spectrum taken at *m/z* = 38 ($H^{37}Cl^+$) does not fit all of the data taken at *m/z* = 36 ($H^{35}Cl^+$).